Oct 26th, 12:00 AM

Component Stiffness Method to Predict Lateral Restraint Forces in End Restraint Single Span Z-Section Supported Roof Systems with One Flange Attached to Sheathing

Michael W. Seek

Thomas M. Murphy

Eighteenth International Specialty Conference on Cold-Formed Steel Structures
Orlando, Florida, U.S.A, October 26 & 27, 2006

Component Stiffness Method to Predict Lateral Restraint Forces in End Restrained Single Span Z-Section Supported Roof Systems with One Flange Attached to Sheathing

Michael W. Seek, PE[1] and Thomas M. Murray, PhD, PE[2]

Abstract

A method is proposed for the prediction of lateral restraint forces in Z-Section supported roof systems with restraints applied at the rafter location. The method incorporates the complex flexural and torsional behavior of the Z-Section and its interaction with the sheathing. The method has been modified using the Finite Element method to account for local deformations. The method shows good correlation with the finite element model and test results.

Introduction

The behavior of Z-sections in roof systems is very complex and subject to many subtleties. Z-sections are typically installed with the top flange attached to sheathing and the bottom flange located at the top of rafter elevation. On low slope roofs, Z-sections have the tendency to roll "uphill" towards the ridge while on roofs with steeper slopes, a Z-section will roll "downhill" towards the eave. Restraints are typically installed at or near the top flange of the Z-section to resist this tendency to rotate. Restraint anchorage is often applied at the supports location because of the ease in which the force can be transferred out of the system.

The prediction of the restraint forces is complex because the principal axes of a Z-section are rotated from the orthogonal planes of loading and restraint. As a result, they are subject to the nuances of unsymmetric bending in which an applied load in the plane of the web induces a lateral deflection. The diaphragm action in the sheathing resists the tendency of the Z-section to deflect laterally,

[1]Graduate Research Assistant, Virginia Tech, Blacksburg, VA, USA.
[2]Montague Betts Professor of Structural Steel Design, Virginia Tech, Blacksburg, VA, USA.

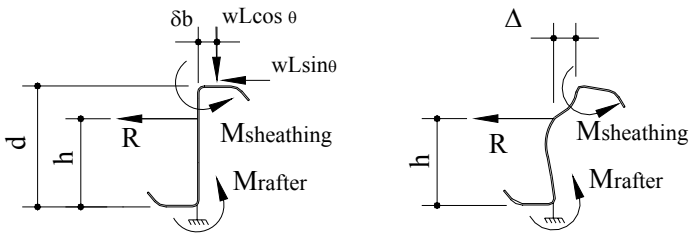

(a) Free Body Diagram (b) Rafter and Sheathing Stiffness

Figure 1 Forces Acting on Z-section

but because it is attached to the top flange of the Z-section, it causes rotation of the Z-section. The bending stiffness of the sheathing helps to resist the rotation of the Z-section but in the process affects the magnitude of the force in the external restraints. The analysis is further complicated by local deformations of the Z-section where large concentrated transverse loads and moments are applied to the relatively thin material. Despite the complexities in analysis, Z-section supported roof systems remain popular due to their efficiency and economy.

Methodology

The magnitude of the restraint force can be found from the free body diagram of the Z-section shown in Figure 1(a). The vertical component of gravity load acts at an eccentricity, δ, along the width of the flange, b, causing a clockwise rotation of the Z-section. This eccentricity is generally accepted to be 1/3 the width of the flange. The downslope component of the gravity load, $w \cdot L \cdot \sin\theta$, acting in the plane of the sheathing causes a counter-clockwise rotation of the Z-section. Deformation of the Z-section generates moments at the connection between the Z-section and the rafter support (M_{Rafter}) and the connection between the Z-section and sheathing ($M_{Sheathing}$). Summing moments about the base of the Z-section, the lateral restraint force becomes

$$R = \frac{wL(\delta b \cos\theta - d \sin\theta) - M_{Sheathing} - M_{Rafter}}{h} \quad (1)$$

A positive restraint force signifies resistance to upslope translation while a negative restraint force signifies resistance to downslope translation.

While the free body diagram is quite simple, determining the magnitude of the moments at the sheathing and rafter is not. A stiffness approach is used to relate the restraint force to the rafter and sheathing moments. Each component of the

system (restraint, rafter, sheathing) generates some force or moment relative to the displacement of the top flange at the restraint location. The stiffness of the restraint, $K_{restraint}$, is the force in the restraint per unit displacement of the top flange. The stiffness of the sheathing, K_{shtg}, and the stiffness of the rafter, K_{rafter}, are the moments in the sheathing or rafter per unit displacement of the top flange. The stiffness of both the sheathing connection and the rafter connection is dependent upon whether the Z-section is directly restrained (a "restrained" Z-section) or restraint is provided indirectly through the sheathing (a "system" Z-section). Thus, there are five components that contribute to the total lateral stiffness of the system: $K_{restraint}$, $K_{shtg,rest}$, $K_{shtg,sys}$, $K_{rafter,rest}$, $K_{rafter,sys}$.

The method assumes that the system of Z-sections has a single degree of freedom. That is, there is some rigid connection linking the displacement at the top of each Z-section in the system. For a through fastened system, this link is provided by the sheathing, while for a standing seam system that permits lateral slip between the sheathing and the Z-section, the rigid link must be provided by some external component such as strapping. As a single degree of freedom, the total stiffness of the system, K_{total}, is the sum of the stiffness of the individual components, or

$$K_{total} = \sum_{n_{rest}} 2K_{rest} + \frac{\sum_{n_{rest}} \left(2K_{rafter,restr} + K_{shtg,restr}\right) + \sum_{n_{sys}} \left(2K_{rafter,sys} + K_{shtg,sys}\right)}{h} \quad (2)$$

where n_{rest} is the number of restrained Z-sections and n_{sys} is the number of system Z-sections. The force generated at the restraint is determined from Equation (3) from the relative stiffness of the restraint to the total stiffnes of all of the components in the system.

$$R = wL\frac{(\delta b\cos\theta - d\sin\theta)}{h} \cdot \frac{\sum K_{rest}}{K_{total}} \quad (3)$$

To develop equations for the stiffness of each of the components, a series of finite element models was performed. The model used was a linear-elastic plate finite element model as described by Seek and Murray (2004a). A total of 282 models were analyzed with three data points taken from each model at roof pitches of 0:12, 3:12 and 6:12. The range of parameters shown in Table 1 was investigated in an attempt to represent the most common systems in use today.

Table 1 Parameters Investigated in Finite Element Analysis

Parameter	Values Tested
Purlin Depth, in (mm)	8 (203), 10 (254), 12 (305)
Purlin Thickness, in. (mm)	0.060 (1.52), 0.097 (2.46), 0.135 (3.43)
Purlin Span, ft, (m)	20 (6.10), 30 (9.14)
Rotational Stiffness of Sheathing Connection, lb-in/ft (N-m/m)	500 (2223), 1000 (4445), 5000 (22,225), 10,000 (44,450)
Diaphragm Stiffness, lb/in (N,mm)	250 (43.8), 1000 (175), 2500 (438), 7500 (1313), 27500 (4816)
Restraint Height	d, 3/4d, 1/2d
Number of Purlins	4, 8

Restraint Stiffness

The stiffness of the restraint is the combination of two sources of deformation at the restraint. The stiffness of the restraint device, K_{device}, is defined as the force at the restraint device relative to the displacement of the device at the height, h, at which the restraint is applied. The configuration stiffness, K_{config}, accounts for the deformation of the Z-section top flange relative to the restraint device. The combination of the two results in the net stiffness of the restraint, K_{rest}.

$$K_{rest} = \frac{\frac{h}{d} K_{device} \cdot K_{config}}{\frac{h}{d} K_{device} + K_{config}} \tag{4}$$

Two basic types of restraint configurations are considered – a discrete restraint and an antiroll device. A discrete restraint is a lateral restraint applied at some discrete location along the height of the Z-section and typically accompanied by flange bolts as shown in Figure 2(a). An antiroll device is considered a device in which the web of the Z-section is clamped to the device with bolts at multiple locations along the height of the Z-section. Bottom flange bolts may or may not be incorporated into an anti-roll device.

To determine the stiffness for a discrete restraint configuration, the web of the Z-section at the restraint was represented by a two dimensional beam model bent about the thickness of the web. To account for the effective width of the web and sheathing in the model, the representative equation was modified based on finite element model results. The resulting configuration stiffness for a discrete restraint per end of restrained Z-section is given in Equation (5).

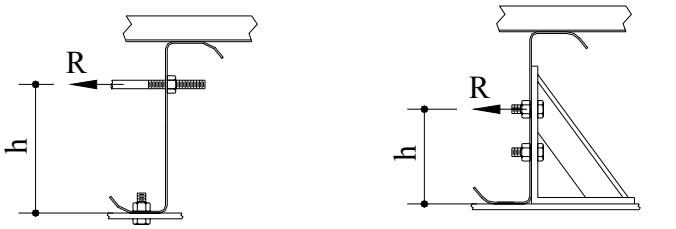

(a) Discrete Restraint (b) Antiroll Device

Figure 2 Restraint Devices

$$. K_{config} = \frac{1/15\, d \cdot (3Et^3)}{h(d-h)^2}\left[\frac{1/15\, d \cdot 2Et^3(3d-h) + L/80 \cdot K_{MDeck} \cdot d(3d-2h)}{1/15\, d \cdot Et^3(4d-h) + L/80 \cdot K_{MDeck} \cdot d(d-h)}\right] \quad (5)$$

An antiroll device is assumed to provide restraint at the location of the top bolt connecting the Z-section web to the antiroll device as shown in Figure 2(b). The stiffness of the configuration for an antiroll device is based on a representative 2- dimensional beam model with a fixed base located at the elevation of the top bolt and a rotational spring at the top flange of the Z-section. This representation is accurate for the case where the antiroll device resists "downhill" displacement of the top flange. For "uphill" displacement of the top flange, the extension of the top of the antiroll clip results in increase in stiffness relative to the downslope case. Because antiroll devices were not included in the finite element analysis, the lower bound approximation considering the downslope case is used. The effective width of the Z-section is assumed to be the width of the antiroll device and the effective width of the sheathing rotational stiffness is taken to be the same as for a discrete restraint. The configuration stiffness for an antiroll device becomes

$$K_{config} = \frac{Eb_{ar}t^3}{(d-h)^3}\left(\frac{L/80\, k_{MDeck}(d-h) + 1/3\, Eb_{ar}t^3}{L/80\, k_{MDeck}(d-h) + 1/12\, Eb_{ar}t^3}\right) \quad (6)$$

Restrained Rafter Stiffness

As there were two restraint configuration stiffness equations to represent the differences between discrete braces and antiroll devices, there are two corresponding rafter stiffness values for each type of restraint. The rafter stiffness for a discrete brace uses the same representative beam model as the discrete restraint configuration with the moment generated at the base of the Z-

section. Because of the nature of the displaced shape, an upslope displacement (positive) generates a negative moment at the rafter, consequently the rafter is assigned a negative stiffness, that is

$$K_{Rafter,rest} = \frac{-0.09 \cdot Et^3 \cdot h}{(d-h) \cdot d} \tag{7}$$

The rafter stiffness for an antiroll device is taken as the moment generated at the point at which the antiroll device is assumed to fix the web of the Z-section - the restraint height, h. Because there is no finite element information or test information available for antiroll devices, it is desirable to underestimate the rafter stiffness. The rotational stiffness of the connection between the Z-section and sheathing is ignored and the effective bending width of the Z-section is taken to be the width of the antiroll device. The rafter stiffness, therefore, for a restrained Z-section at an antiroll device is

$$K_{Rafter,rest} = \frac{\frac{1}{2} Eb_{ar} t^3}{(d-h)^2} \left(\frac{\frac{1}{80} K_{MDeck} (d-h) + \frac{1}{6} Eb_{ar} t^3}{\frac{1}{80} K_{MDeck} (d-h) + \frac{1}{3} Eb_{ar} t^3} \right) \tag{8}$$

System Rafter Stiffness

Two system Z-section configurations are considered for rafter stiffness. The first is the case for the bottom flange of the Z-section bolted to the top flange of the rafter support, referred to as a flange bolted connection. The stiffness is derived from a 2 dimensional beam model fixed at the base and at the top. The rafter stiffness, defined as the moment generated at the base of the Z-section relative to the top flange displacement, is given by

$$K_{Rafter,sys} = 0.45 \frac{Et^3}{2d} \tag{9}$$

The second type of system rafter configuration considered was that of a Z-section with its web bolted to a rafter clip. A rafter clip is considered a single plate extending from the rafter whether the plate is bolted or welded to the rafter. A rafter clip is similar in behavior to an antiroll device although it is not explicitly considered a restraint device in this formulation. The stiffness is defined as the moment at the base of the rafter clip relative to the top flange displacement. The deformation is the combination of the lateral displacement of the rafter clip at the location of the top bolts and the deformation of the Z-section above the rafter clip. The combined stiffness is given by Equation 10.

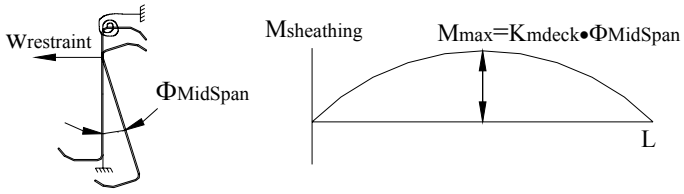

(a) Midspan Displaced Shape (b) Moment Distribution along Length

Figure 3 Sheathing Moment – Rigid End Restraints

$$K_{Rafter,sys} = \frac{E \cdot b_{pl} \cdot {t_{pl}}^3 \cdot t^3}{2t^3\left(h^2(3d-h)\right) + 4{t_{pl}}^3(d-h)^3} \tag{10}$$

Sheathing Stiffness

The moment generated in the sheathing is a function of many factors – the flexural and torsional properties of the Z-section and the diaphragm and bending stiffness of the sheathing. The moment in the sheathing can be quantified using the concept of unrestrained and restoring displacements discussed by Seek and Murray (2005). Considering a Z-section rigidly restrained at each end and ignoring the the bending stiffness of the sheathing, by equating the mid-span lateral unrestrained displacement of the Z-section due to applied forces with the horizontal restoring displacement provided by the sheathing, the uniform restraint provided by the sheathing, $w_{Restraint}$, and the final midspan rotation, $\Phi_{MidSpan}$, can be calculated. by Equations (11) and (12), respectively.

$$w_{Restraint} = w\frac{\dfrac{5\left(\dfrac{I_{XY}}{I_X}\cos\theta\right)L^4}{384EI_{mY}} + \dfrac{(\delta b\cos\theta)d}{2}\dfrac{a^2\beta}{GJ} + \dfrac{L^2\sin\theta}{8G'Width}}{\dfrac{5L^4}{384EI_{mY}} + \dfrac{d^2}{4}\dfrac{a^2\beta}{GJ} + \dfrac{L^2}{8G'Width}} \tag{11}$$

$$\phi_{MidSpan} = \left(w(\delta b\cos\theta) - w_{Restraint}\frac{d}{2}\right)\frac{a^2\beta}{GJ} \tag{12}$$

In this formulation, the restraints applied at each end of the Z-section rigidly restrain the top flange of the purlin and thus the rotation at each end of the Z-section is zero. It is approximated to vary parabolically to the maximum at midspan. If the bending stiffness of the sheathing is considered, the moment in the sheathing is directly proportional to the rotation of the purlin. The moment

in the sheathing therefore has a parabolic distribution.along the length of the Z-section as shown in Figure 3. The midspan rotation of a Z-section subjected to a parabolic moment distribution along the length is

$$\phi_{parabola} = M_{Max}\frac{\kappa}{GJ} \tag{13}$$

Mmax is the maximum moment at the peak of the parabola (at the Z-section midspan). Because the moment in the sheathing is a function of the rotation,

$$M_{Max} = -K_{MDeck}\cdot\phi_{MidSpan} \tag{14}$$

The net Mid Span rotation becomes

$$\phi_{MidSpan} = \left(w(\delta b\cos\theta) - w_{restra\,int}\cdot\frac{d}{2}\right)\tau \tag{15}$$

and the uniform restraint provided by the sheathing is

$$w_{Re\,stra\,int} = w\frac{5\left(\frac{I_{XY}}{I_X}\cos\theta\right)L^4}{\frac{384EI_{mY}}{} + \frac{(\delta b\cos\theta)d}{2}\tau + \frac{L^2\sin\theta}{8G'Width}} \Bigg/ \frac{5L^4}{384EI_{mY}} + \frac{d^2}{4}\tau + \frac{L^2}{8G'Width} \tag{16}$$

The total moment generated in the connection between the Z-section and sheathing for a Z-section rigidly restrained at each end is

$$M_{Shtg} = -\tfrac{2}{3}L\cdot K_{MDeck}\cdot\phi_{MidSpan} \tag{17}$$

The sheathing moment in Equation (17) is generated as a result of the unsymmetric bending properties of the Z-section. Additional moments are generated if the rigid end restraints are replaced with restraints that permit lateral deflection of the top flange of the purlin at the restraint location. As the restraint permits the lateral translation of the top flange, the Z-section rotates relative to the sheathing, generating a uniform moment in the sheathing as shown in Figure 4(a). Due to the torsional moments along the length of the purlin, there is some rotation of the midspan of the Z-section relative to the end rotation. Similar to the case with rigid end restraints, the additional rotation generates a moment that varies parabolically along the length of the Z-section as shown in Figure 4(b). The resulting displaced shapes and sheathing moment distributions can be superposed as shown in the Figure 4(c).

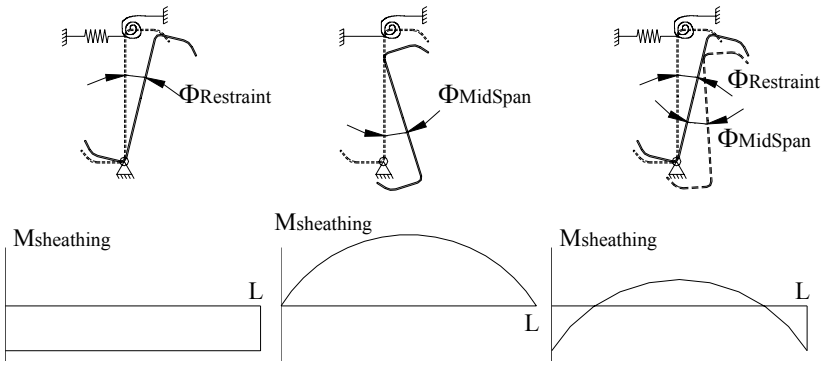

(a) Uniform Moment (b) Parabolic Moment (c) Combined Moment

Figure 4 Sheathing Moment - Z-section with Flexible End Restraints

The magnitude of the uniform moment in the sheathing is equal to

$$M_{uniform} = K_{MDeck}\phi_{restra\,int} = K_{mdeck} \cdot \frac{\Delta_{restra\,int}}{d} \tag{18}$$

Including the effects of the additional uniform moment to the midspan rotation given in Equation (18), the midspan rotation relative to the end rotation becomes

$$\phi_{MS} = \left(w(\delta b \cos\theta) - \frac{w_{restra\,int} d}{2} \right)\tau - \frac{\Delta}{d} K_{MDeck}\tau \tag{19}$$

Equation (16) is used to approximate $w_{restraint}$ for use in Equation (19). A parameter study was performed comparing the exact solution for $w_{restraint}$ considering the effects of the deformation at the restraint with the approximate solution of Equation (16). The difference between the two equations was negligible, warranting the use of the simpler equation. The net moment in the sheathing due to the parabolic distribution becomes

$$M_{Parabola} = \tfrac{2}{3} L \cdot K_{MDeck} \cdot \phi_{MS} \tag{20}$$

Combining the uniform moment and parabolic distribution yields the total sheathing moment

$$Mshtg = \tfrac{2}{3} L \cdot K_{MDeck} \cdot \left(w(\delta b \cos\theta) - \frac{w_{restra\,int} d}{2} \right)\tau + \Delta \frac{L \cdot K_{MDeck}}{d}\left(1 - \tfrac{2}{3} K_{MDeck}\tau\right) \tag{21}$$

The first half of the sum is constant with respect to a given Z-section system while the second varies with respect to the displacement of the top flange of the Z-section. The two components are separated, the former applied as constant moment to the restraint equation and the latter applied as a stiffness term. Considering the second term of Equation (21), the stiffness of the sheathing, defined as the total uniform moment developed in the sheathing per unit lateral displacement of the sheathing becomes

$$K_{shtg} = \frac{L \cdot K_{MDeck}}{d} \lambda \left(1 - \tfrac{2}{3} K_{MDeck} \tau\right) \tag{22}$$

The above formulation is derived using the typical bending assumption that plane sections remain plane. Because Z-sections are a relatively thin material, they undergo substantial local deformations as they undergo these rotations. To account for these local deformations, the multiplier λ, derived from the results of finite element models, is applied.

The sheathing stiffness for a restrained Z-section follows the same format, although the stiffness is increased slightly. There is a local deformation in the region of the restraint that results in a large local rotation between the Z-section web and deck. Consequently there is an increase in the moment in the sheathing near the restraint. The restrained Z-section sheathing stiffness becomes

$$K_{shtg,rest} = \left(\frac{1.43L}{d} + \frac{L_{Fast}}{d-h}\right) K_{MDeck} \lambda \left(1 - \tfrac{2}{3} K_{MDeck} \tau\right) \tag{23}$$

Restraint Force Equation

To include the "constant" sheathing moment, the restraint force in Equation (3) is modified to

$$R = \left(\Sigma wL \cdot \frac{\delta b \cos\theta - d \sin\theta}{h} + \frac{\frac{2}{3} L \cdot K_{MDeck} \lambda}{h} \left(\frac{d}{2} \Sigma w_{restra\,\mathrm{int}} - \Sigma w \cos\theta \cdot \delta b \right) \tau \right) \frac{K_{rest}}{K_{total}} \tag{24}$$

The result of Equation (24) is the force in an individual restraint in a system of purlins. Any number of restraints can be incorporated for any number of purlins. It is assumed that the restraint force between multiple restraints in a bay is distributed according to the relative stiffness of each restraint. Combinations of different purlins with different end conditions can be used in the same bay with the component stiffness method.

A conservative approximation of restraint force for a single restraint in a system can be made by setting the ratio K_{rest}/K_{total} equal to 0.5. For multiple restraints in a homogenous system, the ratio K_{rest}/K_{total} should be set to $0.5/n_{rest}$. This approximation may be further simplified for low slope roofs where $\delta b \cdot \cos\theta > d \cdot \sin\theta$ by approximating $w_{restraint} \sim w \cdot Ixy/2Ix$. For a restraint system that effectively restrains the top flange of the Z-section, these approximations will result in a slightly conservative result on the order of 10%-30%. For a system with a fairly flexible restraint relative to the stiffness of the system, these approximations can lead to an overly conservative approximation of the restraint force greater than 100%.

Several other important quantities may be extracted from this method. The required force per unit length that must be transfered between the sheathing and the Z-section is $w_{restraint}$, given in Equation (16). Along the length of the purlin, this force is nominal. However, at the restraint location, a significant force must be transferred out of the sheathing, through the Z-section and into the restraint. The magnitude of this force is

$$FastenerForce = R\frac{h}{d} + 0.45Lw_{restra\,int} - \frac{wL}{2}\frac{\delta b\cos\theta}{d} \tag{25}$$

Note that this fastener force can be significant and must be transferred over a small distance – a tributary panel width that this force can be expected to be transferred is approximately 12 in. (300 mm) either side of the restraint location.

To check the effectiveness of a bracing system the deformation of the system can be calculated. Based on this method, in general as a Z-section is allowed to displace, the calculated restraint force decreases. The method does not account for any second order effects, therefore displacements should be minimized, particularly at the restraint location. The lateral deflection of the top flange of the Z-section at the restraint location can be approximated by

$$\Delta = \left(\Sigma wL \cdot \frac{\delta b\cos\theta - d\sin\theta}{h} + \frac{\frac{2}{3}L \cdot K_{MDeck}\lambda}{h}\left(\frac{d}{2}\Sigma w_{restra\,int} - \Sigma w\cos\theta \cdot \delta b\right)\tau \right) K_{total}^{-1} \tag{26}$$

With a flexible diaphragm, lateral deflection of the Z-section mid-span relative to the restraints is expected. The midspan lateral deflection of the diaphragm can be approximated as

$$\Delta = \Sigma\left(w_{restra\,int} - w\sin\theta\right)\frac{L^2}{8G'\Sigma Width \cdot} \tag{27}$$

The midspan rotation, Φ_{MS}, of the Z-section relative to the end rotation as shown in Figure 3(c) can be approximated by Equation (19).

Comparison of Prediction Method with Tests and Finite Element Models

In Figure 5, the restraint force predicted using the component stiffness method is plotted on the vertical axis relative to the restraint force from finite element model analysis plotted on the horizontal axis. The solid diagonal line represents an exact 1 to 1 correlation between the prediction method and finite element model while each dashed line represents a 20% deviation from exact correlation. The data points represent all of the finite element models from which the method was derived as discussed in the methodology section.

The equations are compared to full scale laboratory tests by Seek and Murray (2004b) in Figure 6 . The testing program consisted of full scale tests of Z-section roof systems with two, four and six Z-section lines with both through fastened and standing seam sheathing. The Z-sections were tested on pitches

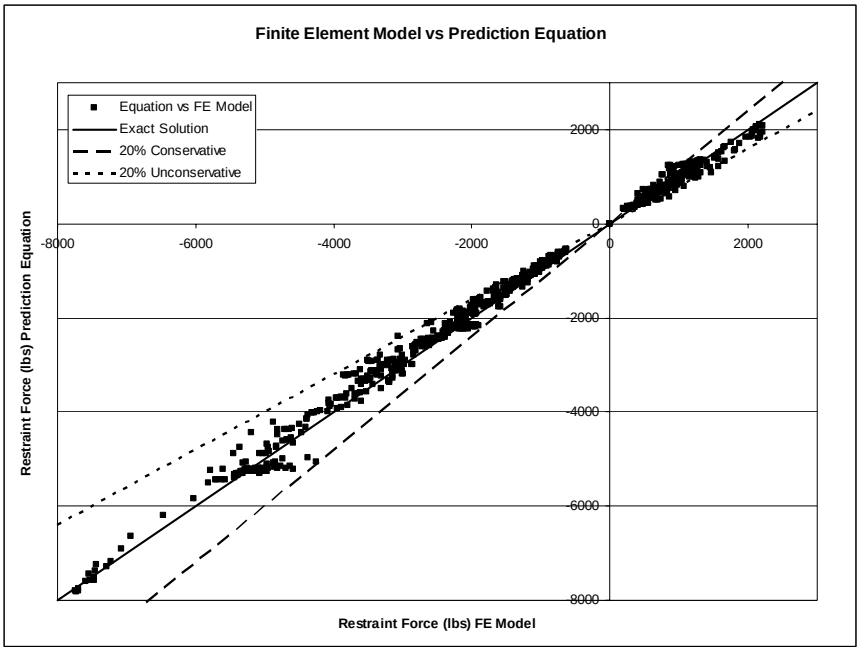

Figure 5 Comparison of Prediction Method with Finite Element Results

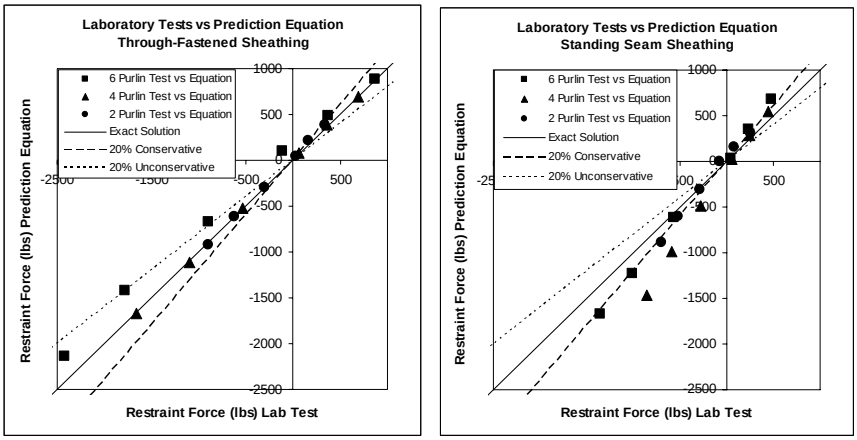

(a) Through Fastened Sheathing (b) Standing Seam Sheathing

Figure 6 Comparison of Prediction Equation with Laboratory Tests

ranging from 0:12 to 4:12. Restraint was applied by a ½ in. diameter rod attached to the web at 2.25 in. from the top of the Z-section.

The prediction method is compared to the results of the through fastened tests in Figure 6 (a). The results of the two and four Z-section line tests correlate well with the prediction method, falling almost exactly on the predicted line. For the six Z-section line tests, the force predicted by the equations is less than that of the test. In the test, a backing plate was placed between the anchorage and the Z-section to reduce local deformations. This backing plate effectively increases the stiffness of the restraint, which would lead to higher restraint forces than predicted. In the case where an unconventional system such as the backing plate is used, a simple test of the configuration could be used to determine the actual stiffness of the configuration.

Comparison of the prediction method with the results of the standing seam tests by Seek and Murray (2004b) are shown in Figure 6 (b). The tests show greater deviation from the prediction equations although the deviation is consistently conservative. Because a standing seam system with an articulating clip was used for the test, 1/2 in diameter rods connected each purlin at the restraint location provide a means to transfer the restraint force through the system,. The prediction method assumes this system to be rigid when in reality it has some flexibility. Consequently, the actual restraint stiffness of the test (or any real system) is less than rigid and the prediction method will always predict the

restraint force conservatively, although in this case the deformation will be underestimated.

Conclusions

The component stiffness method for the determination of lateral brace forces in single span Z-purlin roof systems outlined here is a complex solution to the complex problem of Z-purlin behavior. The method approximates the behavior of Z-section roofs as a single degree of freedom system and attempts to quantify the contribution of all of the components of the system that resist the tendency of the Z-section to rotate and deflect laterally. While complex, the methodology has the ultimate flexibility to accommodate a wide array of system configurations. Because the method is based on stiffness principles, actual stiffness values of components not explicitly quantified herein may be determined from tests and substituted for the equations provided.

Acknowledgements

This study was funded in part by the American Iron and Steel Institute and the Metal Building Manufacturers Association, as well as the Virginia Tech Department of Civil and Environmental Engineering, Via Fellowship Program.

Appendix - References

Seek, M. W. and Murray, T. M. (2004a). "Computer Modeling of Sloped Z-Purlin Supported Roof Systems to Predict Lateral Restraint Force Requirements." *Conference Proceedings, 17th International Specialty Conference on Cold-Formed SteelStructures.* Department of Civil Engineering, University of Missouri-Rolla. Rolla, Missouri.

Seek, M. W. and Murray, T.M. (2004b). "Testing of the Lateral Restraint Force Requirements of Sloped Z-Purlin Supported Standing Seam and Through-Fastened Roof Systems with Two, Four and Six Purlin Lines." Research Report CE/VPI-ST-04/01. Department of Civil and Environmental Engineering, Virginia Polytechnic Institute and State University, Blacksburg, VA, 67 Pages.

Seek, M.W. and Murray, T.M. (2005) Mechanics of Lateral Brace Forces in Z-Purlin Roof Systems. *Conference Proceedings, Structural Stability Council Annual Stability Conference*. Structural Stability Research Council. University of Missouri-Rolla. Rolla, Missouri.

Appendix – Notation

$$I_{mY} = \frac{I_X I_Y - I_{XY}^2}{I_X} \qquad a = \sqrt{\frac{EC_W}{GJ}} \qquad \lambda = \frac{0.71\,¼\,Et^3}{0.38K_{MDeck}d + 0.71\,¼\,Et^3}$$

$$\tau = \frac{\frac{a^2\beta}{GJ}}{1 + \frac{K_{MDeck}}{GJ}\kappa} \qquad \beta = \frac{L^2}{8a^2} + \frac{1}{\cosh\left(\frac{L}{2a}\right)} - 1$$

$$\kappa = \frac{8a^4}{L^2}\left(1 - \cosh\left(\frac{L}{2a}\right) + \frac{\cosh\left(\frac{L}{a}\right) - 1}{\sinh\left(\frac{L}{a}\right)}\sinh\left(\frac{L}{2a}\right)\right) + \frac{5L^2}{48} - a^2$$

b = width of Z-section top flange (in) (mm)
b_{ar} = width of anti-roll clip (in) (mm)
b_{pl} = width of single plate rafter clip (in) (mm)
d = depth of Z-section (in) (mm)
E = modulus of elasticity (29,500,000 psi) (203,400 MPa)
G = shear modulus (11,200,00 psi) (77,200 MPa)
h = height of applied restraint measured from base of Z-section parallel to web (in)
K_{MDeck} = combined rotational stiffness of sheathing and the connection between the Z-section and sheathing (lb-in/ft) (N-m/m)
L = span of Z-section (ft) (m)
L_{Fast} = Spacing between fasteners connection Z-section to Sheathing
n_{sys} = number of system Z-sections
n_{rest} = number of restrained Z-sections
t = thickness of Z-section (in)
t_{pl} = thickness of single plate rafter clip (in) (mm)
w = uniform loading on Z-section (lb/ft) (N/m)
Width = Tributary width of diaphragm (perpendicular to Z-Section Span) per Z-section.(in) (mm)
δ = load eccentricity on Z-section top flange (1/3)
θ = angle between the vertical and the plane of the web of the Z-section (degrees)